0026-895X/06/7003-838–850$20.00
MOLECULAR PHARMACOLOGY
Vol. 70, No. 3
25346/3133109
Mol Pharmacol 70:838–850, 2006
Printed in U.S.A.

Mutagenesis within Helix 6 of the Human β_1-Adrenergic Receptor Identifies Lysine^{324} as a Residue Involved in Imparting the High-Affinity Binding State of Agonists

Omeima Zeitoun, Noel M. Delos Santos, Lidia A. Gardner, Stephen W. White, and Suleiman W. Bahouth

Department of Pharmacology, the University of Tennessee Health Sciences Center, Memphis, Tennessee (O.Z., N.M.D., L.A.G., S.W.B.); and Department of Structural Biology, St. Jude Children's Research Hospital, Memphis, Tennessee (S.W.W.)

Received April 4, 2006; accepted June 5, 2006

ABSTRACT

Competition binding isotherms for agonists to G protein-coupled receptors (GPCR) display high and low binding affinities. Mutagenesis of lysine at position 324 in helix 6 of the wild-type (WT) human β_1-adrenergic receptor (β_1-AR) generated mutant receptors that had GTP-insensitive single low-affinity binding sites for agonists and reduced potencies of full or partial agonists in stimulating adenylyl cyclase. Unlike the WT β_1-AR, intrinsic activities of full and partial agonists in activating the Lys$^{324}\rightarrow$Ala β_1-AR (K324A) mutant were correlated with their binding affinities to the K324A mutant. In assays, such as agonist-mediated phosphorylation and recycling, the K324A mutant and the WT β_1-AR behaved similarly. However, in fluorescence resonance energy transfer assays that determined the proximity between the WT β_1-AR or the K324A mutant to $G_s\alpha$, there were significant differences. The conceptual framework of the ternary complex model could not adequately account for the behavior of the K324A mutant except under assumptions of low receptor-G protein binding affinities. The single low-affinity binding site of the K324A mutant to isoproterenol was converted by the C-terminal 11-amino-acid peptide of $G_s\alpha$, which acts a GDP-bound $G_s\alpha$ mimic, to high- and low-affinity sites. Based upon the three-dimensional architecture of the human β_1-AR, the distance between Lys^{324} and the Asp/Glu-Arg-Tyr motif in helix 3 was the shortest among the various amino acids in helix 6. These findings indicate that Lys^{324} lies in a groove between helices 3 and 6, and its mutagenesis generates a mutant receptor with very low binding affinity for the GDP-bound isoform of G_s.

GPCRs are key bridging molecules between extracellular stimuli such as hormones and neurotransmitters and intracellular signaling cascades. Receptors are multidomain molecules with separate entities for ligand binding, G protein activation, desensitization, and sequestration (Gether et al., 2002). Ligand-activated receptors activate their respective G proteins by promoting the exchange of GTP for GPD bound to the α subunit of the heterotrimer (Gether and Kobilka, 1998). GTP for GPD exchange causes the liberation and dissociation of α-GTP from $\beta\gamma$ complexes that in turn activate the effector enzyme (Bourne, 1997).

The observation that agonists, but not antagonists, stabilize an active conformation of the receptor is based on classic theories of receptor activation. This active receptor conformation consists of the agonist, the receptor, and the G protein in a ternary complex that promotes the biological response (De Lean et al., 1980). The proportion of receptors with this active conformation is determined by means of competition radioligand binding assays in which a constant concentration of a radiolabeled antagonist competes with increasing concentrations of the full agonist. These two-site binding isotherms are then analyzed by nonlinear regression to estimate the population of receptors that display high affinity for the agonist versus those with low affinity. The percentage of receptors that display high-affinity equates the active form of the receptor with a ternary complex involving the agonist, the receptor, and the G protein (Stiles et al., 1984). The percentage of receptors with low-affinity equates

This work was supported by grants from the Southeast Affiliate of the American Heart Association (to S.W.B.) and the American Lebanese Syrian Associated Charities (to S.W.W.). The confocal microscopy facility is supported by National Institutes of Health grant S10-RR13725.

Article, publication date, and citation information can be found at http://molpharm.aspetjournals.org.

doi:10.1124/mol.106.025346.

ABBREVIATIONS: GPCR, G protein-coupled receptor; β_1-AR, β_1-adrenergic receptor; HEK, human embryonic kidney; DMEM, Dulbecco's modified Eagle's medium; WT, wild type; ICYP, iodocyanopindolol; FITC, fluorescein isothiocyanate; FRET, fluorescence resonance energy transfer; YFP, yellow fluorescent protein; CFP, cyan fluorescent protein; GppNHp, guanosine 5′-[β-γ-imido]triphosphate; TCM, ternary complex model.

those receptors that are uncoupled from the G protein and consequently unable to promote the biological response.

The role of helix 6 has gained prominence as a pivotal helix in transducing agonist binding to the GPCR into activation of the receptor associated G protein heterotrimer (Farrens et al., 1996). This mechanism proposes that agonist-mediated activation of GPCR leads to breaking and establishing of interactions between the Asp/Glu-Arg-Tyr [i.e., (D/E)RY motif] in helix 3 and helix 6 that applies to rhodopsin, the β_2-AR,and other GPCRs (Farrens et al., 1996; Gether et al., 1997; Ballestero et al., 2001). By means of histidine substitutions in helices 3 and 6 of the human β_2-AR and the parathyroid receptor, Sheikh et al. (1999) determined the residues in helix 6 that were capable of forming zinc(II) bridges as those involved in agonist-mediated activation of G_s. However, the zinc(II) bridging method failed to identify residues in helix 6 that were involved in regulating the agonist binding affinity to the β_2-AR. After the publication of this article, the crystal structure of dark-adapted rhodopsin revealed that helices 3 and 6 were extended α-helices that project as an α-helix beyond the sequence that is buried in the lipid core of the membrane (Palczewski et al., 2000). The three-dimensional structure of the human β_1-AR was modeled based upon the crystal structure of rhodopsin to estimate the distances between the various amino acids in helix 6 relative to the (D/E)RY region in helix 3. Based upon these measurements and additional site-directed mutagenesis in helix 6, we identified a residue in helix 6 that is involved in imparting the high-affinity binding characteristics of the human β_1-AR to agonists.

Materials and Methods

Site-Directed Mutagenesis. The Flag-tagged human β_1-AR flanked with HindIII (5′) and EcoRI (3′) sites was cloned into the multiple cloning site in the pUC18 plasmid (Delos Santos et al., 2006). Point mutations in helix 6 were generated by site-directed mutagenesis, using the Transformer system (BD Biosciences, San Jose, CA). The sequences of mutated receptors were verified by dideoxy sequencing, followed by cloning of each mutated full-length β_1-AR cDNA into the mammalian expression vector pCDNA-3.1 (Invitrogen, Carlsbad CA).

Cell Culture and Transient Transfections. HEK-293 cells were cultured in DMEM supplemented with 10% fetal bovine serum until they were ~90% confluent. The WT β_1-AR or its point-mutants in pCDNA 3.1 were transiently transfected into HEK-293 cells using the Cytofectene reagent (Bio-Rad Laboratories, Hercules, CA) as follows. Plasmid DNA (5 μg) was diluted into 200 μl of DMEM and then mixed with an equal volume of DMEM containing 12 μl of Cytofectene at room temperature for 30 min. Then 4 ml of DMEM was added, and the DNA-lipid complex was layered over the cells for 5 h at 37°C. Then, an equal volume of DMEM + 10% FBS was added to each culture dish, and the cells were cultured for an additional 36 h.

Membrane Preparation. Transiently transfected cells on 10-cm culture plates were washed twice with 10 ml of ice-cold PBS, then scraped from the plates and pelleted by centrifugation at 2000*g* for 10 min. The cell pellets were suspended in 10 ml of hypotonic buffer composed of 20 mM HEPES, pH 7.4, 2 mM $MgCl_2$, 1 mM EDTA, and 1 mM 2-mercaptoethanol supplemented with 10 μg/ml leupeptin and 10 μg/ml aprotinin with or without 1 mM phenylmethylsulfonyl fluoride for 10 min on ice. The cells were transferred into a glass-glass homogenizer and lysed by 30 up-and-down strokes. Cell lysates were centrifuged at 2500*g* for 5 min to pellet the nuclei, and the supernatant was centrifuged at 15,000*g* for 20 min to pellet the membranes. Membrane proteins were resuspended into 50 mM Tris-HCl, pH 7.5, and 10 mM $MgCl_2$ with protease inhibitors.

Radioligand Binding Assays for β_1-AR. Binding of [^{125}I]iodocyanopindolol (ICYP) to 0.5 μg of membranes was measured in 50 mM Tris-HCl, pH 7.4, plus 10 mM $MgCl_2$ binding buffer containing 0.1 mM ascorbic acid for 2 h at 25°C. For saturation binding experiments, ICYP concentrations ranging from 5 to 300 pM were used. From these experiments, the affinity (K_D) and the maximal density of receptors (B_{max}) for ICYP binding to each β_1-AR subtype were generated by parametric fitting of the data using the Prism 4 software (GraphPad, San Diego, CA). For competition binding experiments, 70 pM ICYP was competed with 24 increasing concentrations of unlabeled competitor ranging from 0.1 nM to 10 μM. The IC_{50} (high) and IC_{50} (low) values for isoproterenol were derived from two-compartment competition to the −GTP data. The IC_{50} values were converted to the corresponding K_{IH} (high) and K_{IL} (low) values using the equation

$$K_I = \frac{IC_{50}\ (nM)}{[(1 + \text{concentration of ICYP})/K_D]} \quad (1)$$

Each saturation and competition experiment was performed in triplicate and replicated between three and five times to determine the mean ± S.E. The log-affinity-shift for each β-agonist toward the WT β_1-AR or the K324A mutant construct was calculated as the log of the ratio of K_I/K_H that was derived from four independent determinations.

Cyclic AMP Accumulation and Adenylyl Cyclase Assays. Transiently transfected cells in six-well plates were switched to DMEM + 25 mM HEPES for 2 h. Appropriate concentrations of isoproterenol in DMEM/HEPES, supplemented with a 300 μM concentration of the phosphodiesterase inhibitor 3-isobutyl-1-methylxanthine (IBMX) were added to the cells for 10 min at 37°C. The reaction was stopped by rapid aspiration of the culture medium and addition of 1 ml of 0.1 N concentrations of isoproterenol HCl followed by freezing of the entire plate in liquid nitrogen. Frozen plates were quickly thawed at 65°C to break the cells, and the cell extract was lyophilized. The dry pellet was resuspended in assay buffer, and cyclic AMP was quantified by radioimmunoassay (RIANEN Assay System; PerkinElmer Life and Analytical Sciences, Boston, MA) and expressed as picomoles of cyclic AMP accumulated per minute per milligram of cell protein using a standard curve that was run in parallel.

For the determination of adenylyl cyclase activity, membranes were prepared from transiently transfected cells without phenylmethylsulfonyl fluoride. Fifty micrograms of membrane proteins were incubated in a final volume of 0.1 ml in buffer containing 50 mM Tris-HCl, pH 7.4, 1 mM $MgCl_2$, 10 mM phosphocreatine, 1 mM cyclic AMP, 2 mM mercaptoethanol, 1 mg/ml bovine serum albumin, 0.4 mM EGTA, 2 mg/ml creatine kinase, and 0.2 mM ATP containing 2 μCi of [α-^{32}P]ATP, 1 mM GTP, and increasing concentration of isoproterenol from 0.1 nM to 0.1 mM. The assay was initiated by the addition of membranes and terminated after 10 min. Cyclic AMP that was formed was separated from ATP by column chromatography, and its specific activity was determined as cyclic AMP formed in picomoles per minute per milligram of protein. The amounts of cyclic AMP formed for each condition were divided by the amounts of cyclic AMP generated by 0.1 mM isoproterenol to estimate the percentage ± S.E. of maximal cyclic AMP generated from each β_1-AR construct. The intrinsic activities on WT β_1-AR or the K324A mutant were defined as the ratios for the maximal activation of adenylyl cyclase by a given β-agonist divided by the activation achieved by 0.1 mM isoproterenol. The data are presented as the mean ± S.E. of the intrinsic activity based upon four determinations for each β-agonist toward the WT or mutant β_1-AR.

Intact Cell Phosphorylation and β_1-AR Immunoprecipitation. Cell cultures were switched to phosphate-free DMEM supplemented with 12.5 mM HEPES for 60 min. Then they were incubated

with 100 μCi of $^{32}P_i$/ml for 2 h at 37°C to equilibrate the [^{32}P]ATP pools. The cells were exposed to 1 mM ascorbic acid (control) or 10 μM isoproterenol for 10 min at 37°C, followed by rapid aspiration of this medium. The cells were lysed with 1 ml/plate of ice-cold radioimmunoprecipitation assay + SDS buffer (20 mM Tris-HCl, pH 8.0, 150 mM NaCl, 5 mM EDTA, 1% Triton X-100, and 0.2% SDS supplemented with protease and phosphatase inhibitors) was added. After scrapping, the lysates were sonicated briefly then centrifuged at 14,000*g* for 5 min at 4°C. From the supernatant, two 5-μl aliquots were removed for protein assay. The remaining volume was processed for immunoprecipitation; each step thereafter was conducted at 0–4°C. Equal amounts of cell lysates were incubated with 40 μl of anti-Flag M2 IgG-agarose beads (Sigma, St. Louis, MO) and incubated at 4°C overnight on a rotating platform. The resin was washed five times with 1 ml of ice-cold radioimmunoprecipitation assay buffer, then 100 μl of Laemmli sample buffer containing 20 mM dithiothreitol was added, and the slurry was incubated at 37°C for 40 min to release the IgG-β_1-AR complex from the resin. The proteins were separated by electrophoresis in 10% acrylamide gels containing 0.1% SDS, dried, and exposed to autoradiography. The relative amounts of ^{32}P-incorporated into the β_1-AR band were determined by electronic counting of the gel by the InstantImager (PerkinElmer Life and Analytical Sciences).

Acid Strip Confocal Recycling Microscopy Protocol. HEK-293 cells expressing the FLAG-tagged WT β_1-AR or FLAG-tagged K324A mutant were grown on poly-L-lysine-coated glass coverslips and serum-starved at 37°C for 1 h in DMEM supplemented with 25 mM HEPES, pH 7.4. The receptors were labeled with 5 μg/ml of FITC-conjugated anti-Flag M2 IgG (Sigma) for 1 h at 37°C. Cells were treated with 10 μM isoproterenol for 30 min at 37°C to promote agonist-mediated receptor internalization. The cells were then chilled in 4°C Tris-buffered saline to stop endocytosis and exposed to 0.5 M NaCl and 0.2 M acetic acid, pH 3.5, for 4 min on ice to remove antibody bound to the β_1-AR (Snyder et al., 2001; Gardner et al., 2004; Delos Santos et al., 2006). Cultures were quickly rinsed in warm DMEM supplemented with HEPES, then incubated with a 100 μM concentration of the β-antagonist alprenolol at 37°C for 10, 20, 30, or 45 min. After each time period, the cover slips were rinsed and fixed in 4% paraformaldehyde in 4% sucrose in phosphate-buffered saline, pH 7.4, for 10 min at room temperature.

Analysis of Immunocytochemical Data. All analyses were performed blind to the stimulation history of the culture. Microscope fields had one to three cells displaying generally healthy morphology. Six to ten cells were imaged per culture, and 10 cultures were processed per condition. Confocal fluorescence microscopy was performed on all the slides using Zeiss Axiovert LSM 510 (100 × 1.4 differential interference contrast oil immersion objective). FITC was excited with the argon laser at 488 nm and imaged through the long-pass emission filter at 520 nm. Thresholds were set by visual inspection and kept constant for each condition. Z-stacks of images were exported as TIFF files, and individual sections were analyzed with Zeiss LSM 510 and NIH Image 1.6 software (http://rsb.info.nih.gov/nih-image/) as described in Delos Santos et al. (2006). In confocal recycling assays, the time constants (t) for β_1-AR recycling were determined by fitting the data to a single exponential decay function of the from of

$$y = y_o + Ae^{-t/\tau} \quad (2)$$

In eq. 2, y_o and A are constants. The data represent the mean of the recycling time ± S.E. from five slides, each involving between 6 and 10 cells.

Data Analysis. Quantitative data were summarized and presented as means and S.E. from at least four determinations, each from triplicate experiments. Least-squares linear regression and nonlinear curves were calculated by the Prism 4.05 program (GraphPad) to estimate the K_{act} of each β_1-AR in stimulating the activity of adenylyl cyclase. Statistical comparisons between samples were analyzed by analysis of variance with Duncan's post hoc test using Prism 4.05 software.

Fluorescence Resonance Energy Transfer Microscopy. These experiments were performed on fixed cells using the sensitized emission method (Kenworthy, 2001). The coding sequences of the Flag-tagged WT β_1-AR or the K324A mutant were amplified by polymerase chain reaction using synthetic oligonucleotides to introduce a 5′ HindIII site followed by the coding sequence and then by a 3′ BamHI site. The amplification primers for the β_1-AR were: forward, 5′-AAGCTTATGGACTACAAGGACGACGATGACAAGGGCGCGGGGGTGCTCGTCCTGGGCG; reverse, TGGATCCACCTTGGATTCCGAGGCGAAGCC. The resulting 1.5-kilobase HindIII-BamHI cDNA was fused in-frame 5′ to the yellow fluorescent protein (YFP) coding sequence in the pECYFP-N1 vectors (BD Biosciences, San Jose, CA) to generate N-terminal fusions of each β_1-AR to YFP. The $G_s\alpha$-cyan fluorescent protein (CFP) vector (Hynes et al., 2004) was provided by C. Berlot (Weis Center for Research, Geisinger Clinic, Danville, PA).

HEK-293 cells were transfected with the desired plasmids using the Lipofectamine reagent (Invitrogen) for 24 h, then plated on poly-L-lysine-covered coverslips for 24 h. The coverslips were exposed to either 1% ascorbic acid or 10 μM isoproterenol for 10 min at 37°C, then fixed with 4% paraformaldehyde, pH 7.4, and mounted onto glass slides in Fluoromount G mounting media (Electron Microscopy Sciences, Hartfield, PA). Coverslips were sealed with clear nail polish and imaged within 24 h after fixation.

Sensitized Emission FRET Microscopy. FRET was recorded using the three-channel sensitized emission mode (Gordon et al., 1998). Donor channel for the CFP was acquired using donor excitation (λ = 458 nm) and donor emission (λ = 475–525 nm) BP filter. Acceptor channel (YFP) was acquired using acceptor excitation (λ = 514 nm) and emission (λ = 530 nm) LP filter. FRET was acquired using excitation (λ = 458 nm) and emission (λ = 530 nm) LP filter. Images were taken from donor, acceptor, and FRET samples. Donor and acceptor images were used to evaluate the cross-talk of signals that is caused by image settings and fluorophore properties. The same acquisition parameters were used for donor, acceptor, and FRET samples. The LSM 510 FRET Macro tool was used to calculate normalized FRET (FRET*N*) values. FRET*N* is a measure of FRET that is normalized for the concentrations of donor and acceptor fluorophores and therefore represents a fully corrected measure of FRET (Gordon et al., 1998). Quantitative comparisons of different FRET methods, has determined that FRET*N* provides the most accurate measure of FRET efficiencies (Gu et al., 2004). In this method, the corrected FRET value for each pixel is calculated and then divided by concentration values for donor and acceptor. FRET*N* was calculated on a pixel-by-pixel basis for the entire image and in regions of interest (marked by rectangles) using the equation of Gordon et al. (1998).

$$\text{FRET}N = \frac{\text{FRET1}}{\text{Dfd} \times \text{Afa}} \propto \frac{[\text{bound}]}{[\text{total d}] \times [\text{total a}]} \quad (3)$$

The equation indicates the proportional (∝) relationship between FRET*N* and the concentrations of the interacting and noninteracting species. In the equation, [bound] represents the concentration of interacting pairs of donor labeled species and acceptor labeled species. The values for [total d] and [total a] represent the total concentrations (interacting and noninteracting) of the donor and acceptor labeled species, respectively. FRET1 is proportional to the FRET signal from the specimen; Dfd is the donor signal that would take place if no FRET occurred and is therefore proportional to the total concentration of donor; and Afa is the acceptor signal that would take place if no FRET occurred and is therefore proportional to the total concentration of acceptor.

Donor and acceptor coefficients were determined in the beginning of each experiment and were kept the same throughout. Donor, acceptor, and FRET thresholds were set to determine the back-

ground value. Threshold values were subtracted from all pixels before FRET calculations. Extreme values were excluded from both the FRET image as well as data table calculation. FRET*N* images are presented in pseudocolor mode.

Molecular Modeling of the Human β_1-AR. Homology modeling was performed with the program SegMod (Levitt, 1992). The program was used to optimally align the sequences of the human β_1-AR and bovine rhodopsin, and then the sequence of the β_1-AR was threaded onto the rhodopsin structure based upon the 1F88 (Palczewski et al., 2000) model of rhodopsin oligomers deposited in the Protein Data Bank. The resulting homology model was then refined according to SegMod protocols. The figures were produced using MOLSCRIPT and rendered with RASTER3D (Merrit and Bacon, 1997), which was also used to estimate the distances in Ångstroms between the various amino acids.

Results

The crystal structure of bovine rhodopsin showed that helices 3 and 6 of rhodopsin were extended α-helices that projected into the cytoplasm further than expected from hydropathy-based computer models (Palczewski et al., 2000). Thus, many residues that were previously assigned to intracellular loop 3 of rhodopsin actually constituted the cytoplasmic neck of helix 6. Among these are a pair of conserved lysine residues that would occupy locations one turn apart in putative helix 6 (Fig. 1). The arrangement of this pair of lysines to the same side of the 6th α-helix is conserved in the majority of class A GPCRs, such as α- and β-adrenergic receptor families, dopamine receptors, and others. To examine whether these residues are involved in GPCR-mediated events, we mutagenized Lys^{321} and Lys^{324} in the human β_1-AR into three different amino acids. Each lysine was mutated to glutamic acid (Lys→Glu) to fully reverse its charge, to methionine (Lys→Met) to neutralize its charge and to mimic its protonated state with an amino acid of similar mass, and to alanine (Lys→Ala) to fully remove the functionality of the side chain. These constructs were transiently transfected into HEK-293 cells, and the binding parameters for each mutant were compared with that of the WT β_1-AR (Table 1). The densities of the β_1-AR (K_D) in each cell line were comparable and ranged from 0.9 to 1.2 pmol/mg of protein. The affinities of [^{125}I]ICYP to the WT β_1-AR or to the mutants were comparable and ranged from 19 to 28 pM ($p > 0.05$), which is similar to the affinity of ICYP to this β-AR subtype. These data indicate that mutagenesis of either lysine did not alter the binding characteristics of these receptors to antagonists.

Binding Characteristics of the WT β_1-AR versus the $Lys^{321/324}$ Mutants. To determine the binding characteristics of each of these receptors to β-agonists, competition of ICYP binding to membranes prepared from each cell line by isoproterenol in the absence of GTP were performed (Fig. 2A). As expected, the competition of ICYP binding to the WT β_1-AR by isoproterenol was shallow, and its parameters were estimated by fitting the data into a two-site binding model. Using these analyses, we estimated the two affinity states of the receptor (K_{IH} = 2 ± 0.14 nM; K_{IL} = 0.35 ± 0.02 μM) and the ratio of the high- versus the low-affinity receptor was 44 to 54%. Mutagenesis of Lys^{321} to the various amino acids described earlier had no significant effects on the high and low affinities of these receptors to isoproterenol or the proportion of low to high β_1-AR populations (Table 1). Mutagenesis of Lys^{324} to any of the three amino acids described before had significant effects on isoproterenol competition isotherms, whereby the data could be fitted into a one-site model with a single low binding affinity K_i of ~0.3 to 1.3 μM. Therefore, mutagenesis of Lys^{324} eliminated the high-affinity binding component to agonists without affecting the binding parameters of antagonists.

When the stable GTP analog guanosine 5′-[β-γ-imido] triphosphate (GppNHp) was present in the competition experiment between isoproterenol and ICYP binding to membranes expressing the WT β_1-AR, the binding isotherm was shifted to the right and displayed a single low-affinity binding state to isoproterenol (Fig. 2A). The affinity of the WT β_1-AR in the presence of GppNHp was 0.35 ± 0.07 μM, the same as the K_{IL} for isoproterenol and close to the affinity of the Lys^{324} β_1-AR mutants in binding to isoproterenol (Fig. 2A). Thus, in accordance with classic paradigm governing the law of mass action for receptor activation, guanyl nucleotides mediated the conversion of the WT β_1-AR from its high-affinity state into a low-affinity state (presumably uncoupled from the G protein). GppNHp, however, did not affect the binding parameters of isoproterenol to the Lys^{324} β_1-AR mutants, indicating that these receptors were insensitive to GTP-mediated uncoupling of the receptor from the G proteins.

Activation of Adenylyl Cyclase by the WT β_1-AR versus the $Lys^{321/324}$ Mutants. First, we determined the effect

GPCR	Helix (VI)					GPCR	Helix (VI)				
hß$_1$-AR	LREQ	K$_{321}$	AL	K$_{324}$	TLGI	boRHO	ATTG	K$_{245}$	AE	K$_{248}$	EVTR
hß$_2$-AR	LKEH	K	AL	K	TLGI	hM$_1$-R	FSLV	K	EK	K	AART
hα$_{1α}$-AR	SREK	K	AA	K	TLGI	hM$_2$-R	PPPS	K	EK	K	KTRT
hα$_{1b}$-AR	SREK	K	AA	K	TLGI	hM$_3$-R	MSLV	K	EE	K	AAQT
hα$_{1C}$-AR	SREK	K	AA	K	TLGI	hM$_4$-R	QMAA	R	ER	K	KVTR
hα$_{1d}$-AR	SREK	K	AA	K	TLAI						
						hADN$_1$-R	KYYG	K	EL	K	IAKS
hDOP$_1$-R	KRET	K	VL	K	TSLV	hADN$_2$-R	KQEV	K	AA	K	SLAI
hDOP$_2$-R	KDHP	K	IA	K	IFEI						
						5HT$_{1A}$-R	ARER	K	TV	K	TLGI
hANG$_{II}$-R	TLIW	K	AL	K	KAYE	5HT$_{1B}$-R	ARER	K	AT	K	TLGI

Fig. 1. Alignment of a conserved pair of lysines within helix VI of different members of class A GPCR. The conserved lysines within helix 6 of the various GPCR are boxed. The abbreviations used are as follows: hα-AR, human α-adrenergic receptor; hβ-AR, human β-adrenergic receptors; hD-R, human dopamine receptor; hANG$_{II}$-R, human angiotensin$_{II}$; boRHO, bovine rhodopsin; hM-R, human muscarinic receptor; hADN-R, human adenosine receptor; h5HT-R, human serotonin receptor.

of mutagenesis of Lys^{321} and Lys^{324} on the ability of the mutated β_1-AR to increase the concentration of cyclic AMP in cells in response to isoproterenol and on the coupling the β-AR to adenylyl cyclase. Basal levels of cyclic AMP formation for the WT β_1-AR were equivalent to those of the Lys^{321} mutants but considerably higher than those of Lys^{324} mutants. For example, basal cyclic AMP for the WT β_1-AR was 14 ± 1.5 pmol/mg of protein, whereas in the K324A mutant, these levels were 4 ± 1 pmol/mg ($p < 0.02$). Basal cyclic AMP levels in the the K324A mutant were not significantly different from their levels in cells expressing empty pcDNA 3.1 (5 ± 2 pmol/mg).

The EC_{50} for the accumulation of cyclic AMP in response to increasing concentrations of isoproterenol was 7 ± 1.5 nM for the WT β_1-AR, and between 9 and 13 nM ($p > 0.05$) for the Lys^{321} or Lys^{324} mutants (Fig. 3, A and B). Cyclic AMP accumulation in response to 100 nM isoproterenol in cells expressing the WT β_1-AR was ~80 pmol/min/mg of protein, and these levels were consistently ~20% higher from those attained in cells expressing either the Lys^{321} or the Lys^{324} mutants (Fig. 3, A and B).

Basal levels of adenylyl cyclase activity in membranes prepared from cells expressing the WT β_1-AR were 18 ± 3 pmol/mg/min, whereas in cells expressing either the K324A mutant or the empty pcDNA vector, these levels were 7 ± 2 pmol/mg/min ($p < 0.05$). Basal adenylyl cyclase levels increased to 300 ± 47 pmol/mg/min upon exposing any of the three types of membranes to 10 μM forskolin. The EC_{50} for the activation of adenylyl cyclase activity in membranes expressing the WT β_1-AR was 0.1 ± 0.02 μM, whereas the EC_{50} for the K324A mutant was 10-fold higher at 1.2 ± 0.3 μM (Fig. 3C). Therefore, the lower basal levels of adenylyl cyclase activity in membranes expressing the K324A mutant were associated with a 10-fold reduction in the coupling affinity of the K324A mutant to adenylyl cyclase activation, but this mutant receptor was still capable of maximally activating the cyclase (Fig. 3C). These data indicate that ligand-independent coupling of the receptor to G_s was obliterated in the K324A mutant even though this construct retained its ability to activate G_s in response to agonists.

Validation of the Assumptions of Ternary Complex Model in Accounting for the Properties of the Lys^{324} β_1-AR Mutant. The TCM is the most widely used model to describe the activation of GPCR. As shown in Fig. 4A, the TCM is concerned with three species, the agonist, [A], the receptor, [R], and the G protein, [G], and assumes that the

TABLE 1

Ligand binding parameters of the wild-type and mutants of the β_1-AR

Site directed mutagenesis of Lys^{321} and Lys^{324} to the amino acids indicated in the table was performed as described under *Materials and Methods*. [^{125}I]ICYP binding was determined as described under *Materials and Methods* on membranes derived from HEK-293 cells expressing the wild-type β_1-AR or the different β_1-AR mutants. Saturation binding experiments were analyzed by nonlinear regression to determine the equilibrium dissociation constant (K_D) of ICYP to each receptor and the receptor density in each membrane preparation. In HEK-293 cells, cell receptor densities for each β_1-AR construct were comparable and ranged from 850 to 1100 fmol of receptor/mg of protein. Competition binding isotherms were analyzed using the two-site competition algorithms in the Prism 4.0 program. When the binding data were best described by two affinity states, K_{IH} and K_{IL} indicate the dissociation constants for the high- and low-affinity state of the receptor, respectively. The results are the mean of four to six independent determinations each in triplicate.

Plasmid Construct	Substituted Amino Acid	Charge at pH 6.0–7.0	Charge Type/Mass	K_D	K_{IH}	K_{IL}	% High-Affinity Sites	% Low-Affinity Sites
				nM	*nM*	*μM*		
Wild type β_1-AR	Lys	Basic (+)	Hydrophilic (polar)/146	19 ± 5	2 ± 0.14	0.35 ± 0.02	44 ± 6	54
K321E	Glu	Acidic (−)	Hydrophilic (polar)/174	29 ± 8	4.2 ± 0.3	0.35 ± 0.03	42 ± 5	58
K321M	Met	Neutral	Hydrophobic nonpolar/149	24 ± 6	4.7 ± 0.4	0.7 ± 0.07	45 ± 8	56
K321A	Ala	Neutral	Hydrophobic nonpolar/89	21 ± 4	5.3 ± 0.4	0.5 ± 0.04	46 ± 5	54
K324E	Glu	Acidic (−)	Hydrophilic (polar)/174	21.4 ± 4		0.87 ± 0.03		100
K324M	Met	Neutral	Hydrophobic nonpolar/149	21.6 ± 4		1.1 ± 0.2		100
K324A	Ala	Neutral	Hydrophobic nonpolar/89	28.6 ± 7		1.3 ± 0.4		100

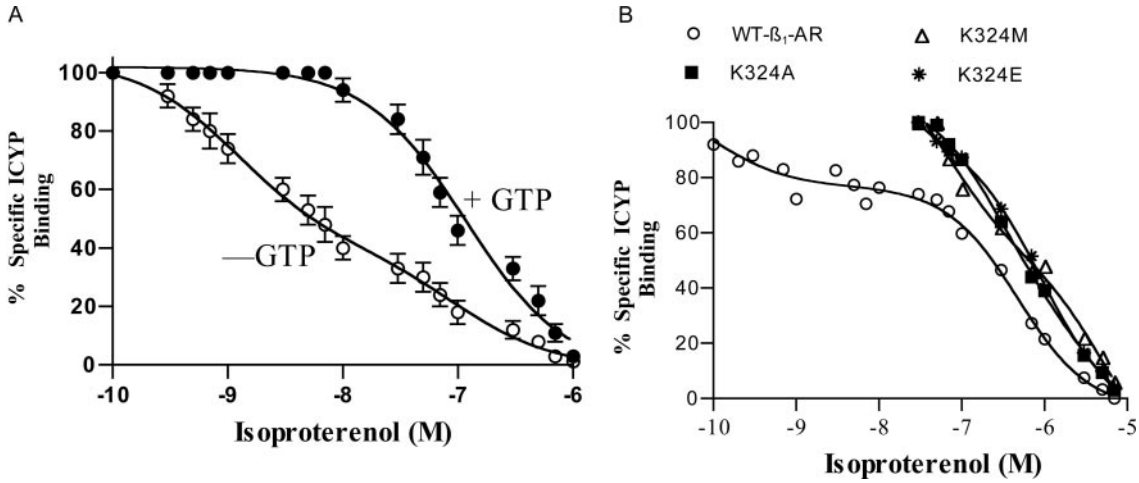

Fig. 2. Competition binding isotherms of isoproterenol on membranes expressing the WT β_1-AR (A) or the Lys^{324} β_1-AR mutants (B). [^{125}I]ICYP binding was determined as described under *Materials and Methods* on membranes derived from HEK-293 cells expressing the wild-type β_1-AR or the Lys^{324} β_1-AR mutants. A, the competition isotherms were determined in either the absence (−GTP) or presence of 100 μM Gpp(NH)p (+GTP). B, the competition isotherm for the WT β_1-AR (−GTP) was plotted on the same plot as the competition isotherms for the indicated Lys^{324} β_1-AR mutants (−GTP). The results are representative of three to five experiments whose mean ± S.E. values are reported in Table 1.

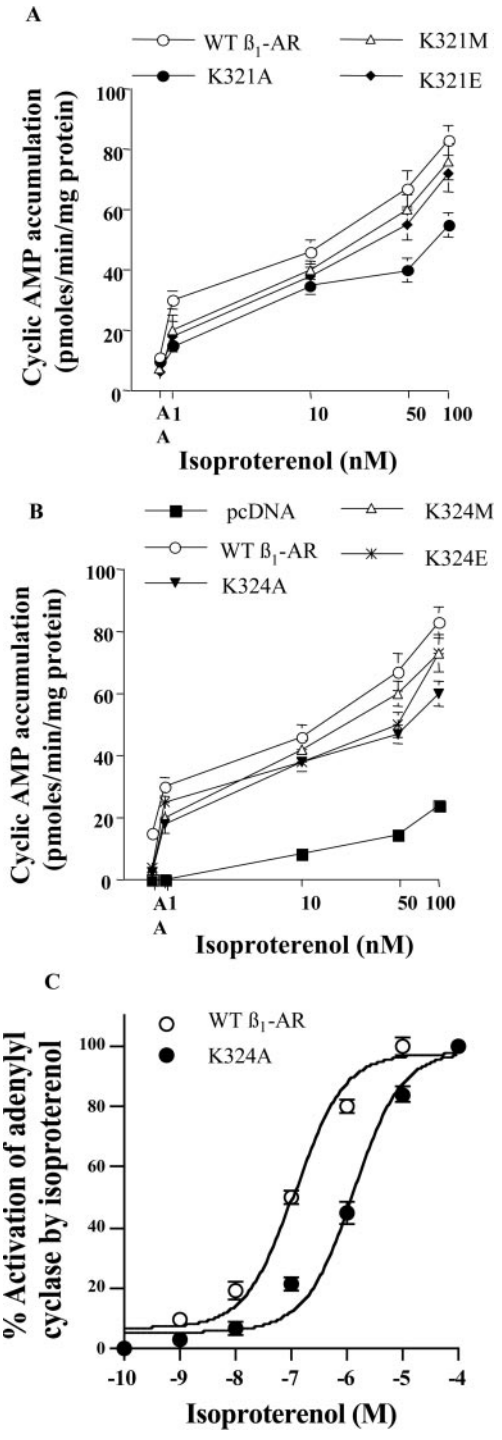

Fig. 3. Effect of mutagenesis of Lys^{321} or Lys^{324} in the β_1-AR on isoproterenol mediated increase in cyclic AMP accumulation or adenylyl cyclase activation. A and B, cells were transiently transfected with the empty mammalian expression vector (pCDNA), the WT β_1-AR or the various Lys^{321}- or Lys^{324}-β_1-AR mutant constructs. The receptor densities in the cells transfected with the various β_1-AR constructs ranged from 850 to 1100 fmol of receptor/mg of protein. Shown are the basal levels of cyclic AMP in the presence of 1 mM ascorbic acid (AA) or in the presence of 1, 10, 50, and 100 nM isoproterenol that were determined as described under *Materials and Methods*. For the Lys^{321} β_1-AR mutants, the results are the means of two independent experiments, whereas for the Lys^{324} β_1-AR mutants, the results are the means ± S.E. of four independent determinations, each in duplicate. C, isoproterenol-mediated activation of adenylyl cyclase in membranes prepared from cells expressing the WT β_1-AR or the K324A mutant were compared. The EC_{50} for the WT β_1-AR was 0.1 ± 0.02 μM, and the EC_{50} for the K324A mutant was 1.2 ± 0.3 μM ($*p < 0.05$, $n = 5$).

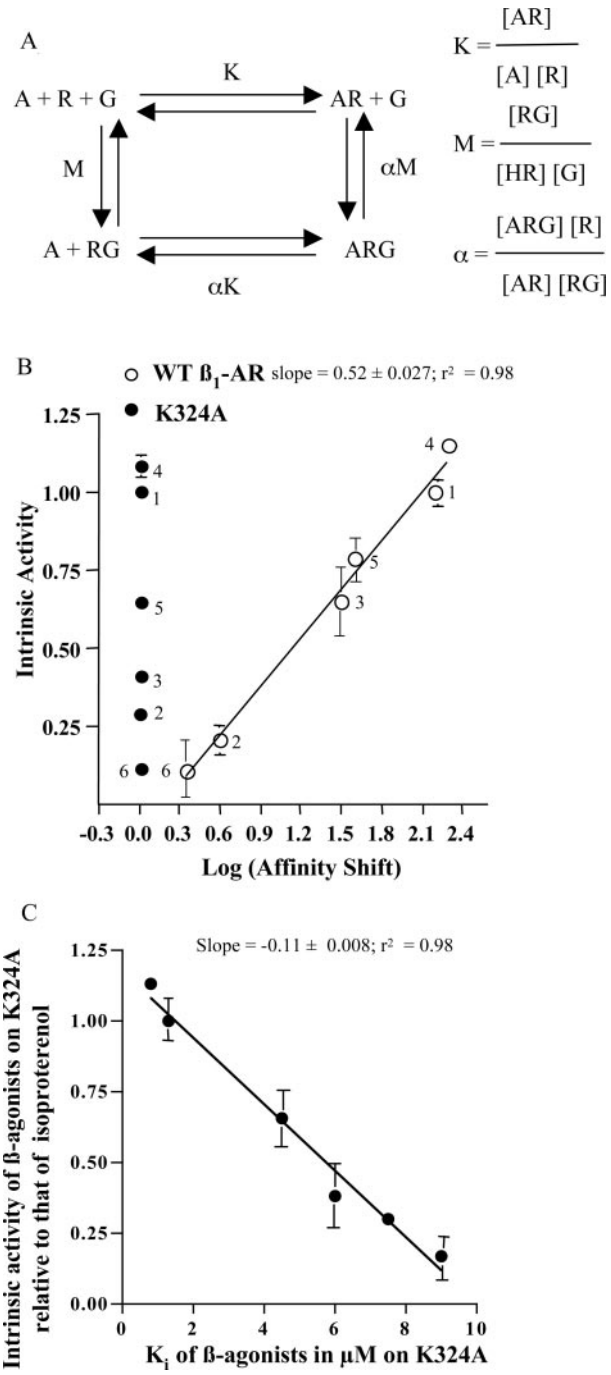

Fig. 4. Correlation between the affinity of various drugs for competing for ICYP binding for the K324A mutant versus the WT β_1-AR as a function of their intrinsic activities for each receptor. A, classic form of the ternary complex model. A, agent; R, receptor; G, G protein. These molecules interact with the equilibrium dissociation constants K, M, αM, and αK as described in De Lean et al. (1980). B, the K_I of different drugs determined by competition for the binding of [^{125}I]ICYP on membranes expressing either the wild-type β_1-AR or the K324A mutant was determined as described under *Materials and Methods*. The "affinity shift" is the ratio between apparent low and high affinities for the K324A mutant and the WT β_1-AR. The "intrinsic activity" for each adrenergic agent was derived as illustrated in the legend of Table 2. The results are the mean of three to five independent determinations, each in triplicate. C, micromolar K_I values of different drugs that were determined by competition for the binding of [^{125}I]ICYP on membranes expressing the K324A mutant were plotted against the "intrinsic activity" of each agent to the K324A mutant. The correlation coefficient for the linearity of the data in A and B was determined using Prism 4.05 software. Isoproterenol, 1; dobutamine, 2; norepinephrine, 3; epinephrine, 4; isoetharine, 5; terbutaline, 6.

active form of the GPCR consists of a ternary complex of [ARG] (De Lean et al., 1980). These species react via four equilibrium reactions that are governed by the law of mass action and are described by three affinity constants. The three affinity constants are M, α, and K. M describes the ligand-independent interaction of the receptor with the G protein. α, also called the coupling constant, is the ratio between the affinities of [A] for the two forms of the receptor [R] and [RG], which reflects the ability of [A] to promote the formation of the [ARG] complex (Kent et al., 1980). K is the affinity constant that describes the affinity of [A] in binding to [R] in the absence of [G]. The value of K is not related to the α coupling constant, indicating that the drug affinity and intrinsic activity (i.e., the maximal physiological response for a given agonist) are not correlated (Samama et al., 1993).

A fundamental assumption of the TCM, therefore, is that the log value of α and the intrinsic activity are correlated (Kent et al., 1980). The value for α is determined in competition isotherms between a constant concentration of the labeled antagonist and increasing concentrations of agonist, followed by estimating the two binding affinities using two-site modeling algorithms (Kent et al., 1980). To determine whether the WT β_1-AR and/or the K324A mutant adhered to the assumptions of the TCM, we examined the ligand binding properties of a series of full and partial agonists. First, we determined the intrinsic activity of each drug in membranes expressing either the WT β_1-AR or the K324A mutant as the ratio of its maximal activation of adenylyl cyclase to that attained by the prototypic full agonist isoproterenol (Table 2). The affinities of each drug for the WT β_1-AR or the K324A mutant were then determined by competition experiments between each drug and a fixed concentration of [^{125}I]ICYP (Table 2). The intrinsic activity of each compound for the WT β_1-AR was plotted as a function of its log-affinity shift for the WT β_1-AR (Fig. 4A). A very significant correlation ($r^2 = 0.98$) was found between the intrinsic activity of each compound for the WT β_1-AR and the extent of its log-affinity shift (Fig. 4A). Therefore, the WT β_1-AR obeyed the assumptions of the TCM model for these drugs. When we examined the data for the K324A mutant, we found that none of the drugs tested displayed a significant log-affinity shift toward the K324A mutant (Table 2 and Fig. 4A). Therefore, a plot of the intrinsic activity versus log shift in affinity for the K324A mutant was non linear, indicating that mutagenesis of Lys^{324} in the human β_1-AR interfered with the ability of receptor-mediated activation of adenylyl cyclase to obey the assumptions of the TCM. The K324A mutation promoted the formation of a single low-affinity binding site that was insensitive to GTP. Under these conditions, the TCM predicts that the affinity of [A] to [R] that is described by the value of the equilibrium binding constant (K) in Fig. 4A, for the various β-adrenergic agents in binding to the K324A mutant might be correlated with their intrinsic activity. Therefore, we plotted the K_I values for the six β-adrenergic agonists in competing for ICYP binding to membranes expressing the K324A mutant versus their intrinsic activities toward the K324A mutant (Fig. 4C). These values were correlated, indicating that the K324A mutant behaved as predicted by the TCM under conditions of G $\sim$ 0 or low probability of [R] + [G] to spontaneously form [RG], which is reflected by the value of M (Fig. 4A).

There are other interesting observations concerning the high-affinity binding site for agonists in GPCR, in that the proportion of these sites can be increased by high molar excesses of synthetic peptides corresponding to the carboxyl-terminal region of the $G_s\alpha$ subunit (Palm et al., 1990; Rasenick et al., 1994). The generation of the high-affinity binding site in cells or membranes is thought to involve the binding of the $G_s\alpha$ carboxyl-terminal peptide to a region in the β-AR that is involved in generating the high-affinity state of the receptor to agonists (Rasenick et al., 1994). Through this mechanism, these peptides presumably engage the receptor molecules and convert them into a high-affinity state for agonists.

Our first goal was to replicate these findings in membranes prepared from cells expressing the WT β_1-AR. For this purpose, the membranes were preincubated with a 200 μM concentration of the 11-mer $G_s\alpha$ carboxyl-terminal peptide or a control scrambled peptide, then the binding of [^{125}I]ICYP to these membranes was competed with increasing concentrations of isoproterenol. The data in Fig. 5 show that in the presence of the control peptide, 48 $\pm$ 7% of the WT β_1-AR displayed a high-affinity state of 1.6 nM for isoproterenol. In the presence of the $G_s\alpha$ carboxyl-terminal peptide, the proportion of WT β_1-AR that displayed the high-affinity state almost doubled to $\sim$90 $\pm$ 7%, but their affinity (1.6 nM) was

TABLE 2

Ligand binding parameters of adrenergic agents to wild-type and K324A β_1-AR

Competition of [^{125}I]ICYP binding by each drug was determined as described under *Materials and Methods* on membranes derived from HEK-293 cells expressing the wild-type β_1-AR or K324A. Cell receptor densities for the WT-β_1-AR were 1050 $\pm$ 180 fmol of receptor/mg of protein and for K324A they were 985 $\pm$ 110 fmol of receptor/mg of protein. Competition binding isotherms were analyzed using the two-site competition algorithms to estimate the means $\pm$ S.E. for the K_{IH} and K_{IL} for each drug. These data were derived from three to five determinations, each performed in triplicate. The 'affinity shift' for the WT β_1-AR was calculated as the ratio between the apparent binding affinity for the low affinity binding site (K_L) relative to the high affinity binding site (K_H), which were derived from four independent competition determinations. The affinity shift for K324A was similarly calculated from four independent competition experiments. To calculate the 'intrinsic activity' for each adrenergic agent, membranes were prepared from cells expressing either WT β_1-AR or K324A. Adenylyl cyclase activation in 50 μg of each type of membrane by increasing concentrations of each β-agonist was determined as described under *Materials and Methods*. The intrinsic activity indicates the ratio between maximal adenylyl cyclase activation in picomoles per minute per milligram of protein elicited by each drug to that obtained with the full agonist isoproterenol. The results are the mean of three to five independent determinations each in triplicate. These data were used for plotting the data in Fig. 4, B and C.

β-Adrenergic Agent	Competition Data WT β_1-AR		Log Affinity Shift for WT β_1-AR	Intrinsic Activity for WT β_1-AR	K_I for K324A	Log Affinity Shift for K324A	Intrinsic Activity for K324A
	K_{IH}	K_{IL}					
	nM	μM			μM		
Isoproterenol (1)	2 $\pm$ 0.15	0.35 $\pm$ 0.02	2.2	1.0	1.3 $\pm$ 0.2	0	1.0
Dobutamine (2)	660 $\pm$ 14	3.2 $\pm$ 0.6	0.6	0.21 $\pm$ 0.02	7.5 $\pm$ 3	0	0.3 $\pm$ 0.03
Norepinephrine (3)	8.8 $\pm$ 1.5	0.35 $\pm$ 0.04	1.5	0.65 $\pm$ 0.07	6.0 $\pm$ 0.38	0	0.38 $\pm$ 0.04
Epinephrine (4)	5 $\pm$ 1	0.92 $\pm$ 0.07	2.3	1.15 $\pm$ 0.11	0.8 $\pm$ 0.15	0	1.13 $\pm$ 0.06
Isoetharine (5)	21 $\pm$ 2	1.0 $\pm$ 0.2	1.6	0.79 $\pm$ 0.11	4.5 $\pm$ 1	0	0.66 $\pm$ 0.02
Terbutaline (6)	220 $\pm$ 34	0.53 $\pm$ 2	0.35	0.11 $\pm$ 0.01	9 $\pm$ 1.4	0	0.17 $\pm$ 0.01

similar to that of the K_{IH} of the WT β_1-AR in the presence of control peptide or in membranes expressing the WT β_1-AR (Table 1). Therefore, the $G_s\alpha$ peptide acted as a G_s mimic to increase the proportion of high-affinity binding sites without altering the affinity (K_{IH}) of the WT β_1-AR. Next, we tested the effect of these peptides on membranes expressing the K324A mutant (Fig. 5). In the presence of the control peptide, these membranes displayed a single low-affinity binding site of K_I = 1 μM. However, in the presence of the $G_s\alpha$ carboxyl-terminal peptide, it was evident that the isoproterenol competition curves were shallow. Analysis of the competition isotherms indicated that these curves were best fitted into a two-site model with a K_{IH} of 3 nM (42%) ($p > 0.05$ between the K_{IH} of the WT β_1-AR and K_{IH} of the K324A mutant plus $G_s\alpha$ peptide) and a K_{IL} of 1 μM (58%) for isoproterenol. We tested the effect of these peptides on basal and isoproterenol-stimulated adenylyl cyclase activities in membranes expressing WT β_1-AR or the K324A mutant, but these experiments were not feasible because $G_s\alpha$ carboxyl-terminal peptides inhibit isoproterenol-mediated activation of adenylyl cyclase in permeabilized cells and membranes because they compromise the normal coupling of the agonist-activated receptor to G_s (Rasenick et al., 1994).

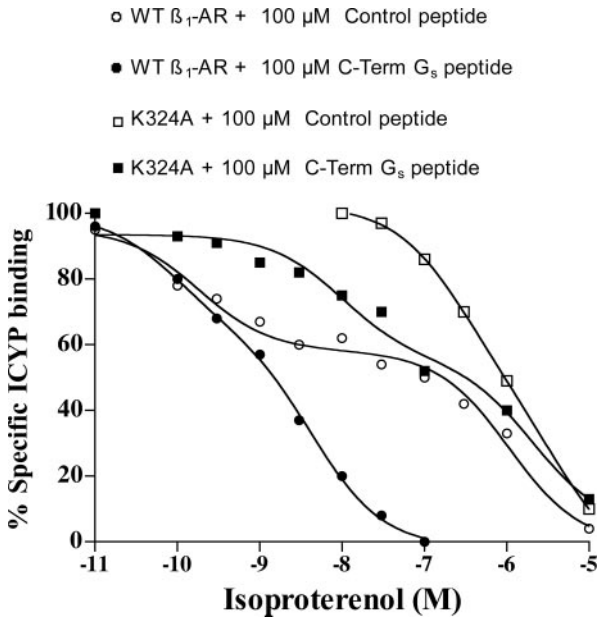

Fig. 5. Effect of the $G_s\alpha$ carboxyl-terminal peptide on the competition binding isotherms of isoproterenol on membranes expressing WT β_1-AR or the K324A mutant. [^{125}I]ICYP binding was determined as described under *Materials and Methods* on membranes derived from HEK-293 cells expressing the wild-type β_1-AR or the K324A mutant. The competition isotherms were determined in either the presence of 200 μM of an 11-amino-acid control peptide (Arg-Gln-Leu-His-Leu-Met-Glu-Tyr-Leu-Gln-Arg) or in the presence of a 200 μM concentration of the 11-amino carboxyl-terminal $G_s\alpha$ peptide (Gln-Arg-Met-His-Leu-Arg-Gln-Tyr-Glu-Leu-Leu). Analysis of the isoproterenol-competition binding isotherms resulted in a K_{IH} of 1.6 nM (R_H = 48%) and K_{IL} of 1.4 μM (R_L = 52%) for the WT β_1-AR in the presence of control peptide. In the presence of the carboxyl-terminal $G_s\alpha$ peptide, the data for isoproterenol competition of ICYP binding to the WT β_1-AR could be fitted into a single site with a K_I of 1.6 nM. Competition of ICYP binding to membranes expressing the K324A mutant in the presence of the control peptide could be fitted into a single low-affinity binding site with a K_I of 1 μM. In the presence of the carboxyl-terminal $G_s\alpha$ peptide, the data for isoproterenol competition of ICYP binding to the K324A mutant could be confidently fitted into a two-site model with a K_{IH} of 3 nM (R_H = 42%) and K_{IL} of 1 μM (R_L = 58%). The results are representative of three experiments each in quadruplicates.

Characterization of the Distribution and Recycling of the WT β_1-AR and the K324A Mutant by Confocal Microscopy. To investigate whether the K324A mutation affects the localization of the β_1-AR in HEK-293 cells, cells stably expressing the Flag-tagged WT β_1-AR or the K324A mutant were labeled for 1 h at 37°C with FITC-conjugated anti-Flag IgG, then fixed and imaged with the Zeiss LSM-510 (Fig. 6A). The confocal images showed that the WT β_1-AR and the K324A mutant were expressed in the cell membrane (Fig. 6A, a and h). Exposing these cells to isoproterenol for 30 min promoted the internalization of WT β_1-AR into distinct intracellular punctate vesicular structures that are associated with the internalized GPCR phenotype (Fig. 6A, b and i). The cells were then exposed to mild acidic conditions to strip off the FITC-labeled IgG from the surface of the cell to visualize the internalized receptor populations (Fig. 6A, c and j). The images show that isoproterenol promoted equivalent internalization of WT β_1-AR and the K324A mutant. To determine the recycling kinetics of the various β_1-AR constructs, the cells were exposed to the β-antagonist alprenolol to inhibit receptor internalization so that recycling could be accurately measured by the confocal recycling assay. The WT β_1-AR and the K324A mutant recycled rapidly (Fig. 6A, d–g and k–n) with equivalent recycling kinetics of $t_{1/2}$ of 17 $\pm$ 5 min (Fig. 6B). Therefore, mutagenesis of Lys^{324} did not affect the distribution, internalization, or recycling of the K324A mutant.

Characterization of Isoproterenol-Mediated Phosphorylation of WT β_1-AR and the K324A Mutant. Agonist-mediated activation of GPCR is associated with phosphorylation of these receptors, which is a prelude to their desensitization and internalization. We compared basal and isoproterenol-mediated phosphorylation of these receptors in cells expressing equivalent amounts of receptor densities (Fig. 6C). As shown in Fig. 6C, exposure of cells expressing either the WT β_1-AR or the K324A mutant to isoproterenol resulted in receptor phosphorylations that were rapid (maximal response occurred in $\sim$ 3 min) and resulted in a 490 $\pm$ 70% increase in ^{32}P-incorporation above basal levels (n = 4). Therefore, the K324A mutation did not alter either basal or agonist-stimulated phosphorylation of this receptor.

Effect of the K324A Mutation on the Interaction of the β_1-AR with the $G_s\alpha$ Subunit. The K324A mutant displayed a single low-affinity binding site for agonists that we hypothesize resulted from its low affinity toward GDP-G_s. To examine the molecular basis of this intriguing phenomenon, we determined whether the WT β_1-AR interacted differently from the K324A mutant with the $G_s\alpha$ subunit. These interactions were assessed by FRET microscopy, which relies on the transfer of energy from an excited donor CFP to an acceptor YFP that occurs when the two tagged proteins are in very close proximity (<50 Å; Gordon et al., 1998). YFP was fused in-frame downstream from the carboxyl terminus of the β_1-AR. $G_s\alpha$-CFP contains CFP inserted into the α1/αA loop of $G_s\alpha$, the site of alternative splicing of $G_s\alpha$; like WT $G_s\alpha$, it was expressed in the membrane and displayed activity comparable with that of $G_s\alpha$ (Hynes et al., 2004). Before the initiation of FRET, the localization, internalization, and recycling of β_1-AR-YFP in HEK-293 cells was determined by confocal microscopy (Fig. 7A).

To determine the basal magnitude of FRET between the β_1-AR and $G_s\alpha$ in HEK-293 cells, WT β_1-AR-YFP or the

K324A mutant-YFP were transiently transfected with $G_s\alpha$-CFP into HEK-293. The cells were fixed and the normalized FRET*N* technique as measured by the sensitized emission method (Gordon et al., 1998) was used to determine the binding of each receptor to $G_s\alpha$ (Fig. 7B). In the absence of isoproterenol, the WT β_1-AR associated with $G_s\alpha$ with a FRET*N* efficiency of 2.3 ± 1.1%, whereas the FRET*N* efficiency between the K324A mutant and $G_s\alpha$ was not detectable (FRET*N* = 0, n = 3). These data indicate that in unstimulated cells, a small proportion of the WT β_1-AR population were in close proximity to $G_s\alpha$, but within the sensitivity of this FRET assay, close proximity between the K324A mutant and $G_s\alpha$ could not be demonstrated. In cells that were fixed after the addition of 10 μM isoproterenol for 10 min, FRET*N* between the WT β_1-AR and $G_s\alpha$ was 27 ± 2%, whereas the comparable FRET*N* between the K324A mutant and $G_s\alpha$ was 5 ± 1.3% (n = 3, $p < 0.01$). Therefore, in response to isoproterenol-induced conformational changes in the β_1-AR, a large percentage of WT β_1-AR population was in close proximity to $G_s\alpha$, whereas under the same conditions, a comparably much smaller population of the K324A mutant interacted or was in close proximity to $G_s\alpha$.

Three-Dimensional Modeling of the 6th α-Helix of the Human β_1-AR. In Fig. 8, the distribution of Lys^{321} and Lys^{324} in helix 6 relative to the (D/E)RY motif in helix 3 are displayed based upon the crystal structure of dark-adapted bovine rhodopsin (Palczewski et al., 2000). In Table 3, we provide the distance in Å between the α-carbons of the amino acids in the cytoplasmic terminus of helix 6 and the α-carbon in each amino acid of the (D/E)RY sequence in helix 3 of the human β_1-AR. The closest residue to the (D/E)RY motif was Lys^{324}, followed by Leu^{323} and Gln^{320}. Sheikh et al. (1999) probed the microdomains in the β_2-AR that are involved in coupling this receptor to G_s by a zinc(II) bridging method. In this method, each residue in helix 6 was mutated to a histidine. Likewise, Ala^{134} in helix 3 [that lies one turn away from the (D/E)RY motif] was also mutated to a histidine. Therefore, if the distance between the pair of histidines in helices 3 and 6 was <11Å, zinc(II) bridges would form between them. The formation of these zinc(II) bridges would prevent the

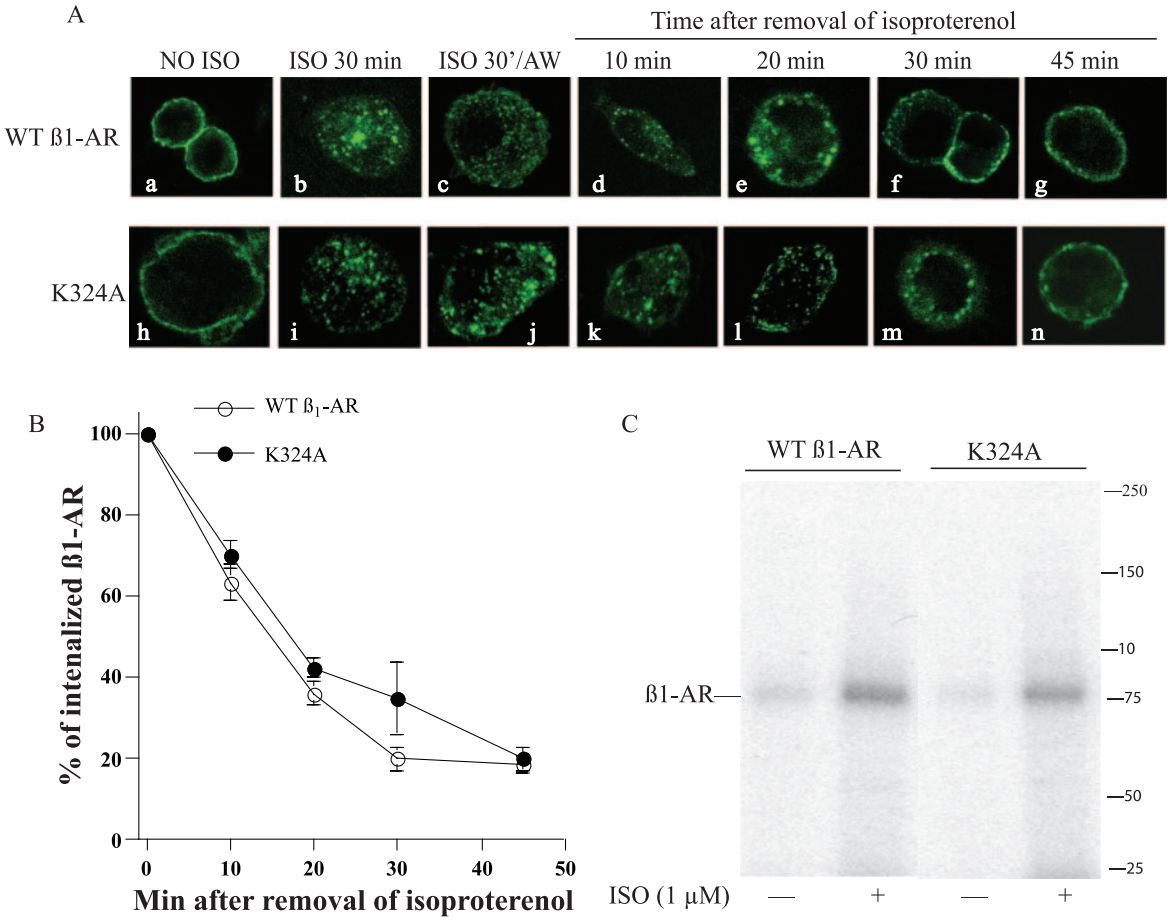

Fig. 6. Characterization of the distribution, internalization, recycling, and phosphorylation of the wild-type β_1-AR versus the K324A mutant. A, HEK-293 cells stably expressing Flag-tagged WT β_1-AR or Flag-tagged K324A mutant were labeled with FITC anti-Flag IgG for 1 h, followed by 10 μM isoproterenol for 30 min. The cells were acid-washed and treated with 100 μM alprenolol for the times indicated in the figure. At the end of each alprenolol time point, the slides were fixed and visualized by confocal microscopy (n = 3). Each scale bar represents 5 μm. B, the LSM-510 software was used to determine the density of the pixels inside the circular boundary whose circumference was delimited 300 nm inside the cell. The pixels inside the boundary in isoproterenol/acid washed cells was set arbitrarily to 100% to indicate 100% internalization and the ratios in alprenolol-treated cells were calculated as a percentage at each time period. The $t_{1/2}$ for recycling was calculated by fitting the relevant data to a single exponential function of time that were described in eq. 2. C, cells expressing the Flag-tagged WT β_1-AR or the Flag-tagged K324A mutant were metabolically labeled with $^{32}PO_4$, then exposed to buffer (ascorbic acid 1%, denoted as – in the figure) or 10 μM isoproterenol for 10 min. The β_1-AR was immunoprecipitated using anti-Flag IgG-agarose and subjected to SDS-PAGE and autoradiography. ^{32}P incorporated into each band were counted electronically using the PerkinElmer InstantImager.

separation of helix 3 from helix 6 in response to agonist-mediated activation of the β_2-AR and therefore, would prevent the activation of G_s that is measured by guanosine 5′-*O*-(3-thio)tri-[^{32}P]phosphate binding to membranes. Under these conditions, it was shown that histidine substitutions of Glu^{268}, His^{269}, and Leu^{272} in helix 6 of the human β_2-AR prevented agonist-mediated activation of G_s as indexed by 5′-*O*-(3-thio)triphosphate binding. The corresponding residues in the human β_1-AR are Glu^{319}, Gln^{320}, and Leu^{323}, which according to the data in Table 3 are separated by <12Å from the (D/E)RY amino acids in helix 3. Sheikh et al. (1999) however, could not identify the residue in helix 6 that was involved in imparting the high-affinity binding of the β_2-AR to agonists. Using pharmacological, biochemical and ultrastructural approaches, we determined that Lys^{324} in helix 6 was involved in this phenomenon and that it was the closest amino acid in helix 6 to the (D/E)RY motif in helix 3.

Discussion

From the effects of mutagenesis of lysine at position 324, we infer that this residue in the human β_1-AR is involved in imparting the high-affinity binding state of the receptor to agonists. This high affinity state is thought to result from the association of the receptor with the appropriate G protein because addition of GTP reduces the agonist binding affinity by promoting the dissociation of the α and $\beta\gamma$ subunits of G_s from the receptor and from each other. These observations were confirmed in mouse lymphoma S49 *CYC*$^-$ cells that genetically lack the α-subunit of G_s and display a single low-affinity binding constant for agonists to the β_2-AR (Haga et al., 1977; Ross et al., 1977). Conversely, the affinity of antagonists to GPCR was not affected by GTP or by the genetic absence of the G protein in *CYC*$^-$ S49 cells. Likewise, the affinity of the K324A mutant for antagonists was similar to the affinity of the WT β_1-AR to these agents. The ability of G proteins to modulate the binding of agonists, but not antagonists, suggests a reciprocal interaction between the receptor-G protein interface and the agonist-binding pocket (Sheikh et al., 1999).

How this reciprocity is mediated is currently unknown. In rhodopsin, light induces a conformational change that enhances the affinity of rhodopsin for the binding of the retinal

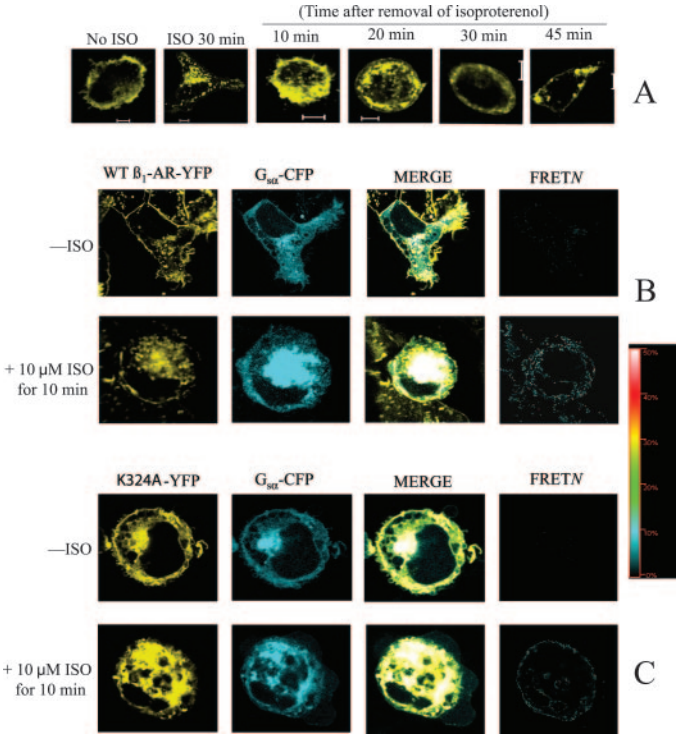

Fig. 7. Sensitized emission FRET microscopy between the WT β_1-AR and the $G_s\alpha$ subunit or the K324A mutant and the $G_s\alpha$ subunit. A, cells expressing WT β_1-AR-YFP were exposed to 10 μM isoproterenol for 30 min to internalize the β_1-AR, then the recycling of the receptor was visualized by confocal microscopy as described in the legend of Fig. 6. B and C, cells coexpressing the WT β_1-AR-YFP and $G_s\alpha$-CFP (B) or the K324A mutant-YFP and $G_s\alpha$-CFP (C) were exposed to ascorbic acid (−ISO) or 10 μM isoproterenol for 10 min at 37°C. The slides were fixed with 4% paraformaldehyde and imaged as described under *Materials and Methods*. FRET*N* is presented in pseudo color. Normalized FRET*N* values were calculated using the LSM510 Macro 1.5 FRET software (with eq. 3) that was described under *Materials and Methods*.

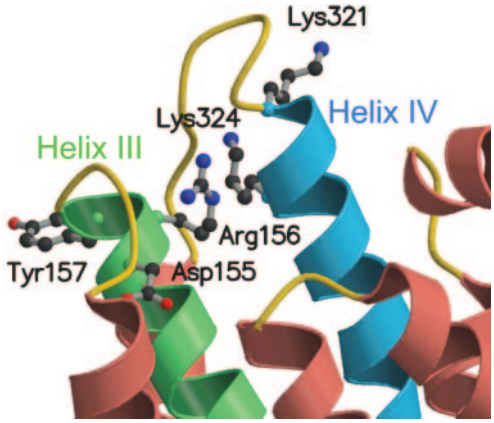

Fig. 8. Structural model of the transmembrane helices of the human β_1-AR based upon the crystal structure of dark-adapted bovine rhodopsin. The amino acids in the transmembrane helices of the human β_1-AR and rhodopsin were aligned according to the three-dimensional data of Palczewski et al. (2000) by the SegMod computer program (Levitt, 1992). Using the aligned sequence of the β_1-AR, we threaded the sequence into that of the rhodopsin structure and refined the structure to build a structurally valid model. The figure was produced using MOLSCRIPT and rendered with RASTER3D computer programs. The figure shows the distribution of the various transmembrane helices of the human β_1-AR. Structural details of the various amino acids in the cytoplasmic termini of helices 3 and 6 were calculated from the coordinates.

TABLE 3

Estimation of the distance between the (E/D)RY motif in helix 3 and the various residues in helix 6 of the human β_1-AR by the three-dimensional model of rhodopsin as described by Palczewski et al. (2000)

The distances were estimated from the SEGMOD-generated three-dimensional image of rhodopsin in Fig. 8.

Residue in Helix 6 of the Human β_1-AR	Distance between the Indicated Residue and the α Carbon of		
	Asp^{155}	Arg^{156}	Tyr^{157}
		Å	
Arg^{318}	15.67	12.31	13.96
Glu^{319}	14.51	11.74	14.11
Gln^{320}	10.74	7.97	10.59
Lys^{321}	11.98	8.61	11.04
Ala^{322}	13.32	10.62	13.74
Leu^{323}	10.10	8.08	11.69
Lys^{324}	9.13	6.33	9.45
Thr^{325}	12.74	10.08	12.95
Leu^{326}	12.49	10.82	14.24

G protein transducin (Zuyga et al., 1994). Transducin in turn stabilizes a spectral form of rhodopsin called metarhodopsin II that is generated after light-mediated "activation" of rhodopsin. The activation of transducin is thought to occur by light-induced movement of helix 6 relative to helix 3 in rhodopsin (Farrens et al., 1996). In analogy to rhodopsin, separation of helix 3 from helix 6 in many GPCRs was identified as the major conformational hallmark of agonist-mediated activation of these receptors (Javitch et al., 1995; Elling et al., 1997; Gether et al., 1997; Ballesteros et al., 2001).

Compared with the WT β_1-AR, membranes expressing the the K324A mutant displayed lower affinity in binding to isoproterenol and displayed significantly lower basal levels of cyclic AMP. Moreover, the EC_{50} for isoproterenol in activating adenylyl cyclase in membranes expressing the K324A mutant was 10-fold higher than its comparable EC_{50} in membranes expressing the WT β_1-AR. These data suggest that separate amino acids might be involved in high-affinity binding to agonists versus agonist-mediated activation of the G protein. Through the engineering of Zn^{2+} binding domains in the human β_2-AR, Sheikh et al. (1999) discovered that amino acids in helix 6 that were in close proximity to the G protein-binding residues in helix 3 were involved in the activation of G_s. Thus, Glu^{268}, His^{269}, and Leu^{271} in helix 6, which were the closest to the (D/E)RY residues in helix 3, were involved in agonist-mediated activation of the G protein, but had no effect on agonist binding affinity. Under these experimental conditions, Lys^{272} in the β_2-AR (which corresponds to Lys^{324} in the β_1-AR) was not involved in either G protein activation or high-affinity binding because its distance from Leu^{134} in helix 3 was estimated to be >12.5 Å (Sheikh et al., 1999). In this report, we show by biochemical, pharmacological, cell biological, and structural criteria that Lys^{324} in involved in imparting high-affinity binding characteristics to agonist. The discrepancy between our data and that of Sheikh et al. (1999) is due mostly to differences in the three-dimensional models that were used and the residues for which distances were calculated. First, Sheikh et al. (1999) relied on the Baldwin three-dimensional model for rhodopsin derived from electron diffraction (Baldwin et al., 1997), which preceded the Palczewski et al. (2000) model derived from X-ray diffraction of rhodopsin crystals to estimate the distances among the various amino acids. Second, we measured the distances between amino acids in helix 6 and the individual (D/E)RY amino acids in helix 3, whereas Sheikh et al. (1999) estimated the distances between the various amino acids in helix 6 and Leu^{134}, which lies one turn away from the (D/E)RY sequence. Our data in Table 3 are derived from a different set of parameters than those used by Sheikh et al. (1999), and we believe our parameters provide a more objective analysis and reveal that Lys^{324} is the closest residue to the (D/E)RY motif among those in helix 6. Nevertheless, both models are consistent with the notion that separate entities in the GPCR are responsible for high-affinity binding and G protein activation through amino acids in helix 6 that lie in close proximity to the (D/E)RY motif in helix 3 (Table 3). Furthermore, a role for Leu^{323} in regulating the coupling of the β_1-AR to the G protein and a role Glu^{318} and Gln^{319} in the $serotonin_{2A}$ receptor (that corresponds to Glu^{319} and Gln^{320} in the β_1-AR) have been established (Lattion et al., 1999; Shapiro et al., 2002).

The TCM was introduced to mathematically model the observation that agonists, but not antagonists, stabilize an activated conformation of the receptor (De Lean et al., 1980). In the TCM, the affinity constant (M) describes the ligand-independent interaction between the receptor and the G protein (Fig. 4A). Our results in Figs. 3 and 4 indicate that basal activity of adenylyl cyclase in the K324A mutant membranes was significantly lower that that in WT β_1-AR membranes. Likewise, basal cyclic AMP accumulation in cells expressing the K324A mutant was significantly less than in cells expressing the β_1-AR. These two pieces of data suggest that the value of M between the K324A mutant and G_s is apparently much less than the value for M between the WT β_1-AR and G_s.

Concerning α, we observed a strong correlation between the drug's intrinsic activity and log α values for competition of these drugs to the WT β_1-AR (Fig. 4B). For the K324A mutant, however, there was no correlation because $\alpha = 1$ (i.e., log $\alpha = 0$). The TCM and the law of mass action both predict that $\alpha \sim 1$ in conditions where the levels of the appropriate G protein are very low, such as in S49 *CYC*$^-$ cells or when experimentally generated in the presence of Gp-p(NH)p (Haga et al., 1977; Ross et al., 1977). Under these conditions, theoretical binding isotherms modeled after the TCM or the law of mass action display a single class of binding sites. Accordingly, our data for the K324A mutant are consistent with the assumption that G is apparently ~ 0. Concerning the third constant (K), which describes the affinity of [A] in binding to [R] in the absence of [G] (Fig. 4A), we found that the affinity of drugs to the WT β_1-AR and their intrinsic activities were not correlated, which is expected. However, for the K324A mutant, there was an excellent correlation between the affinity of a drug in binding to the K324A mutant and its intrinsic activity. Again, our data seem to support the notion that the K324A mutant was behaving as if $G \sim 0$. In the absence of the G protein, the TCM becomes analogous to the so-called allosteric receptor model for a monomeric receptor that was fashionable for interpreting ligand-receptor interactions before the TCM (Thron, 1973; Furchgott, 1978). This model predicts binding curves with unitary slope factors consistent with homogeneous class of binding sites, in which K is the affinity constant that describes the equilibrium constant for

$$[A] + [R] \overset{K}{\rightleftharpoons} [AR]$$

which describes agonist-mediated binding and subsequent activation of the receptor in the absence of [G] (Colquhoun, 1973). In this case, a correlation between the unitary affinity of the receptor and its intrinsic efficacy is observed, which is the case for the K324A mutant.

The situation in cells expressing the K324A mutant is not analogous to a G protein-free system, because immunoreactive levels of the $G_s\alpha$ subunit in cells expressing the WT β_1-AR and the K324A mutant were equivalent (data not shown). The other proviso that can reduce the rate of

$$[AR] + [G] \overset{\alpha M}{\rightleftharpoons} [ARG]$$

is when the affinity of the receptor to the G protein (M) is very low. In this case, the low basal activity of the K324A

mutant as well as its low affinity to the GDP-bound form of the G_s trimer result in unitary affinity binding data because of the poor interaction between the K324A mutant and the GDP-bound G_s trimer. To test this hypothesis, we reasoned that the concentration of G_s in cell membranes should be markedly increased to shift the equilibrium between the free mutant-R and G to into a complex of mutant-RG. We attempted to do that by overexpression of the α-subunit of G_s, but this method did not statistically increase the binding affinity of the K324A mutant to isoproterenol (data not shown). The other method that we tested was based on the observation that the percentage of GPCR that display the high-affinity binding component to agonists can be manipulated by synthetic peptides corresponding to the 11 carboxyl-terminal amino acids of the α-subunit of the G protein. In other words, these peptides increase the probability of [mutant-R] + [G_{mimic}] to form [mutant-RG_{mimic}]. The addition of peptides representing the 11 carboxyl-terminal amino acids of the α-subunit of transducin stabilized the metarhodopsin II state of rhodopsin (Hamm et al., 1988), and the addition of the 11 carboxyl-terminal peptide of $G_s\alpha$, enhanced the affinity of the β_2-AR for binding isoproterenol in permeabilized cells and membranes (Palm et al., 1990; Rasenick et al., 1994). As predicted, the percentage of sites in the WT β_1-AR that displayed high-affinity binding to isoproterenol were increased from approximately 40 to ~90% by the $G_s\alpha$ carboxy-terminal peptide. Interestingly, the single low-affinity binding site model for the K324A mutant in the presence of the control peptide was converted to a statistically valid two-site model for isoproterenol in which the high-affinity binding sites accounted for ~ 42% (Fig. 5). These sites displayed a K_{IH} for isoproterenol equal to the K_{IH} of isoproterenol on WT β_1-AR. Thus, the low-binding affinity of the K324A mutant to isoproterenol was most probably a reflection of low M values for the interaction of the K324A mutant with the GDP-form of G_s. In this regard, the carboxyl-terminal peptide of $G_s\alpha$ mimicked the activity of the GDP bound form of G_s and when the concentration of this GDP-G_s mimic increased, the two-binding affinity states were manifested. These data are strongly in agreement with the data in Figs. 2 and 3 that show low basal activities in cells and membranes expressing the K324A mutant and a 10-fold lower coupling affinity of the K324A mutant compared with the WT β_1-AR.

Our data thus far seem to implicate low [M] values as a potential cause for the single low-affinity site for isoproterenol in binding to the K324A mutant. Because M is the rate constant for the spontaneous formation of [RG] from [R] + [G], and if the stipulation outlined above is true, then the density of [RG] in cells expressing the WT β_1-AR is expected to be greater than its density in cells expressing the K324A mutant. Therefore, we compared, by FRET microscopy, the levels of $G_s\alpha$ that were in close proximity to the WT β_1-AR and those that were close to the K324A mutant in intact cells (Fig. 7). FRET occurs when the distance between donor/acceptor chromophores is <50 Å (Gordon et al., 1998). Thus, by comparing the percentage FRET*N* values between WT β_1-AR-YFP/$G_s\alpha$-CFP versus the K324A mutant-YFP/$G_s\alpha$-CFP, we deduced that the basal levels of the K324A mutant-$G_s\alpha$ heterodimers were significantly lower than WT β_1-AR-$G_s\alpha$ heterodimers ($p < 0.05$). We realize that the strength of the FRET signal is a function of the distance between chromophores, the binding affinity of protein-protein interactions, and chromophore orientation within the complex (Gordon et al., 1998; Kenworthy, 2001; Gu et al., 2004). Although any differences between any of these parameters can affect the intensity of FRET signals between acceptor/donor pairs, this method consistently yielded negligible FRET*N* values between the K324A mutant-YFP and $G_s\alpha$-CFP ($n = 3$) in unstimulated cells. Next, we compared the percentage FRET*N* levels of β_1-AR-YFP:$G_s\alpha$-CFP versus the K324A mutant-YFP:$G_s\alpha$-CFP in cells after the activation of the β_1-AR with isoproterenol. Under these conditions, we speculate that the percentage FRET*N* values will be derived from the formation of [ARG] from [AR] + [G]. Based upon the law of mass action and the TCM, the rate constant for the formation of [ARG] from [AR] + [G] is αM (Fig. 3A). Thus, if our hypothesis concerning M is correct, we would expect to observe lower percentage FRET*N* values between the K324A mutant-YFP/$G_s\alpha$-CFP versus WT β_1-AR-YFP/$G_s\alpha$-CFP, which was what we consistently observed ($n = 3$, $p < 0.05$). We conducted additional experiments to compare the biology of the K324A mutant with that of the WT β_1-AR because we discovered that point mutations of selected amino acids in helix 8 of the human β_1-AR resulted in aberrant distribution and phosphorylation of these receptors (Delos Santos et al., 2006). These analyses indicated that the phosphorylation and internalization of the K324A mutant were comparable with those of the WT β_1-AR (Fig. 6). Thus, fractional occupancy of either the WT β_1-AR or the K324A mutant was apparently sufficient to provide maximal efficacy, which is in agreement with the spare receptor hypothesis for GPCR (Ariens et al., 1964).

The preference for lysine at position 324 in helix 6 in promoting the high-affinity binding for agonists is supported by several independent criteria. Without exception, a lysine amino acid is found in the corresponding position of helix 6 in more than 24 class A GPCRs that are closely related to the β_1-AR (Fig. 1). Modeling of the three-dimensional structure of rhodopsin indicates the existence of a groove between helices 3 and 6 (Palczewski et al., 2000). Within this groove, Lys^{248} of rhodopsin that corresponds to Lys^{324} in the human β_1-AR projects into this space (Palczewski et al., 2000). Based upon these data, our model in Fig. 8 proposes that Lys^{324} projects into the groove between helices 6 and 3 in the direction of the (D/E)RY motif. Thus, if the high-affinity state of the GPCR is due to an association between amino acids in helix 6 with the (D/E)RY motif in helix 3, we speculate that Lys^{324} would participate in such an interaction, because it is the amino acid in helix 6 that is closest to the (D/E)RY residues in helix 3 (Table 3). Furthermore, if the high-affinity state involves additional interactions between helix 6 and those amino acids of the G protein that project into the groove between helices 3 and 6, we expect that Lys^{324} will be involved in that also, because it lies on the side of the 6th α-helix that projects into the space between helices 3 and 6. Two additional pieces of evidence show a potential role of the carboxyl-terminal domain of the α-subunit of G proteins in interacting with selective residues in the groove between helices 3 and 6. First, mapping of rhodopsin-transducin interactions with fluorescent probes revealed a key interaction between the carboxyl terminus of the transducin α-subunit to the inner face of helix 6 (Janz and Farrens, 2004). Second, the crystal structure of dark adapted rhodopsin dimers overlaid with transducin heterotrimers shows that the carboxyl terminus of the transducin α-subunit is inserted deep into the

'groove between helices 3 and 6 of rhodopsin (Filipek et al., 2004). There is anecdotal functional evidence that Lys^{248} in helix 6 of rhodopsin, which corresponds to Lys^{324} in the β_1-AR, is critically important because the substitution of Lys^{248} into a leucine prevented mutant rhodopsin from activating transducin (Franke et al., 1998). Finally, the data in Fig. 5 clearly show a functional relationship between Lys^{324} and the carboxyl-terminal sequence of $G_s\alpha$. Therefore, biophysical, structural and functional analyses of transducin/rhodopsin interactions in-tandem with functional studies, reveal that a lysine residue lies in a privileged position in helix 6 of the GPCR. This residue, when mutagenized, generates a novel class of receptors that affords the perfect opportunity to study the physiological importance of these receptors after knockin into mice lacking the β-adrenergic receptor phenotype (Rohrer et al., 1999).

References

Ariens EJ, Simonis AM, and van Rossum JM (1964) Drug-receptor interaction and relation between stimulus and effect, in *Molecular Pharmacology,* vol 1 (Ariens EJ ed) pp 394–466, Academic Press, New York.

Baldwin JM, Schertler GF, and Unger VM (1997) An alpha-carbon template for the transmembrane helices in the rhodopsin family of G-protein-coupled receptors. *J Mol Biol* **272:**144–164.

Ballestero JA, Jensen AD, Liapakis G, Rasmussen SG, Shi L, Gether U, and Javitch JA (2001) Activation of the β_2-adrenergic receptor involves disruption of an ionic lock between the cytoplasmic ends of transmembrane segments 3 and 6. *J Biol Chem* **276:**29171–29177.

Bourne HR (1997) How receptors talk to trimeric G proteins. *Curr Opin Cell Biol* **9:**134–142.

Colquhoun D (1973) The relation between classical and cooperative models for drug action, in *Drug Receptors* (Rang HP ed) pp 149–182, University Park, Baltimore.

De Lean A, Stadel JM, and Lefkowitz RJ (1980) A ternary complex model explains the agonist-specific binding properties of the adenylate cyclase-coupled β-adrenergic receptor. *J Biol Chem* **255:**7108–7117.

Delos Santos NM, Gardner LA, White SB, and Bahouth SW (2006) Characterization of the residues in helix 8 of the human β_1-adrenergic receptor that are involved in coupling the receptor to G proteins. *J Biol Chem* **281:**12896–12907.

Elling CE, Thirstrup K, Nielsen SM, Hjorth SA, and Shwartz TW (1997) Engineering of metal-ion sites as distance constraints in structural and functional analysis of 7TM receptors. *Fold Res* **2:**S76–S80.

Farrens DL, Altenbach C, Yang K, Hubbell WL, and Khorana HG (1996) Requirement of rigid-body motion of transmembrane helices for light activation of rhodopsin. *Science (Wash DC)* **274:**768–770.

Filipek S, Krzysko KA, Fotiadis D, Liang Y, Saperstein DA, Engel A, and Palczewski K (2004) concept for G protein activation by G protein-coupled receptor dimers: the transducin/rhodopsin interface. *Photochem Photobiol Sci* **3:**628–638.

Franke RR, Sakmar TP, Oparain DD, and Khorana HG (1998) A single amino acid substitution in rhodopsin (lysine 248 to leucine) prevents activation of transducin. *J Biol Chem* **263:**2119–2122.

Furchgott RF (1978) Pharmacological characterization of receptors: its relation to radioligand-binding studies. *Fed Proc* **37:**115–120.

Gardner LA, Delos Santos NM, Matta SG, Whitt MA, and Bahouth SW (2004) Role of the cyclic AMP-dependent protein kinase in homologous resensitization of the β_1-adrenergic receptor. *J Biol Chem* **279:**21135–21143.

Gether U, Asmar F, Meinild AK, and Rasmussen SG (2002) Structural basis for activation of G-protein-coupled receptors. *Pharmacol Toxicol* **91:**304–312.

Gether U and Kobilka BK (1998) G protein-coupled receptors II. Mechanism of agonist activation. *J Biol Chem* **273:**17979–17982.

Gether U, Lin S, Ghanouni P, Ballesteros JA, Weinstein H, and Kobilka BK (1997) Agonists induce conformational changes in transmembrane domains III and VI of the $beta_2$ adrenoceptor. *EMBO (Eur Mol Biol Organ) J* **16:**6737–6747.

Gordon GW, Berry G, Liang XH, Levin B, and Herman B (1998) Quantitative fluorescence resonance energy transfer measurements using fluorescence microscopy. *Biophys J* **74:**2702–2713.

Gu Y, Di WL, Kelsell DP, and Zicha D (2004) Quantitative fluorescence resonance energy transfer (FRET) measurement with acceptor photobleaching and spectral unmixing. *J Microsc* **215:**162–173.

Haga T, Ross EM, Anderson HJ, and Gilman AG (1977) Adenylate cyclase permanently uncoupled from hormone receptors in a novel variant of S49 mouse lymphoma cells. *Proc Natl Acad Sci USA* **74:**2016–2020.

Hamm HE, Deretic D, Arendt A, Hargrave PA, Koening B, and Hoffman KP (1988) Site of G protein binding to rhodopsin mapped with synthetic peptides from the α subunit. *Science (Wash DC)* **241:**832–835.

Hynes TR, Mervine SM, Yot EA, Sabo JL, and Berlot CH (2004) Live cell imaging of G_s and the β_2-adrenergic receptor demonstrates that both α_s and $\beta_1\gamma_7$ internalize upon stimulation and exhibit similar trafficking patterns that differ from that of the β_2-adrenergic receptor. *J Biol Chem* **279:**44101–44112.

Janz JM and Farrens DL (2004) Rhodopsin activation exposes a key hydrophobic binding site for the transducin α-subunit terminus. *J Biol Chem* **279:**29767–29773.

Javitch JA, Fu D, Chen J, and Karlin A (1995) mapping the binding crevice of the dopamine D_2 receptor by the substituted-cysteine accessibility method. *Neuron* **14:**825–831.

Kent RS, De Lean A, and Lefkowitz RJ (1980) A quantitative analysis of beta-adrenergic receptor interactions: resolution of high and low affinity states of the receptor by computer modeling of ligand binding data. *Mol Pharmacol* **17:**14–23.

Kenworthy AK (2001) Imaging protein-protein interactions using fluorescence resonance energy transfer microscopy. *Methods* **24:**289–296.

Lattion A-L, Abuin L, Nenniger-Tosato M, and Cotecchia S (1999) Constitutively active mutants of the β_1-adrenergic receptor. *FEBS Lett* **457:**302–306.

Levitt M (1992) Accurate modeling of protein conformation by automatic segment matching. *J Mol Biol* **226:**507–533.

Merrit EA and Bacon DJ (1997) Raster 3D: photorealistic molecular graphics. *Methods Enzymol* **227:**505–524.

Palczewski K, Kumasaka T, Hori T, Behnke CA, Motoshima H, Fox BA, Le Trong I, Teller DC, Okada T, Stenkamp RE, et al. (2000) Crystal structure of rhodopsin: a G protein-coupled receptor. *Science (Wash DC)* **289:**739–745.

Palm D, Munch G, Malek D, Dees C, and Hekman M (1990) Identification of a Gs-protein coupling domain to the β-adrenergic receptor using site-specific synthetic peptides. *FEBS Lett* **261:**294–298.

Rasenick MM, Watanabe M, Lazarevic MB, Hatta S, and Hamm HE (1994) Synthetic peptides as probes for G protein function. Carboxyl-terminal $G\alpha_s$ peptides mimic G_s and evoke high affinity agonist binding to β-adrenergic receptors. *J Biol Chem* **269:**21519–21525.

Rohrer DK, Chruscinski A, Schauble EH, Bernstein D, and Kobilka BK (1999) Cardiovascular and metabolic alterations in mice lacking both β_1- and β_2-adrenergic receptors. *J Biol Chem* **274:**16701–1670.

Ross EM, Maguire ME, Sturgill TW, Biltonen RL, and Gilman AG (1977) Relationship between the beta-adrenergic receptor and adenylate cyclase. *J Biol Chem* **252:**5761–5775.

Samama P, Cotecchia S, Costa T, and Lefkowitz RJ (1993) A mutation-induced activated state of the β_2-adrenergic receptor: extending the ternary complex model. *J Biol Chem* **268:**4625–4636.

Shapiro DA, Kristiansen K, Weiner DM, Kroese WK, and Roth BL (2002) Evidence for a model of agonist-induced activation of 5-hydroxytryptamine$_{2A}$ serotonin receptors that involves the disruption of strong ionic interaction between helices 3 and 6. *J Biol Chem* **277:**11441–11449.

Sheikh SP, Vilardrage J-P, Baranski TJ, Lichtarge O, Iiri T, Meng EC, Nissenson RA, and Bourne HR (1999) Similar structures and shared switch mechanisms of the β_2-drenoceptor and the parathyroid hormone receptor. Zn(II) bridges between helices III and VI block activation. *J Biol Chem* **274:**17033–17041.

Snyder EM, Philpot BD, Huber KM, Dong X, Fallon JR, and Bear MF (2001) Internalization of ionotropic glutamate receptors in response to mGluR activation. *Nat Neurosci* **4:**1079–1085.

Stiles GL, Caron MG, and Lefkowitz RJ (1984) Beta-adrenergic receptors: biochemical mechanisms of physiological regulation. *Physiol Rev* **64:**661–743.

Thron CD (1973) On the analysis of pharmacological experiments in terms of an allosteric receptor model. *Mol Pharmacol* **9:**1–9.

Zuyga TA, Fahmy K, and Sakmar TP (1994) Characterization of rhodopsin-transducin interaction: a mutant rhodopsin photoproduct with a protonated Schiff base activates transducin. *Biochemistry* **33:**9753–9761.

Address correspondence to: Suleiman W. Bahouth, Department of Pharmacology, The University of Tennessee Health Sciences center, 874 Union Avenue, Memphis, TN 38163. E-mail: sbahouth@utmem.edu